Search for Ultralight Dark Matter with Spectroscopy of Radio-Frequency Atomic Transitions

Xue Zhang,[1] Abhishek Banerjee,[2] Mahapan Leyser,[1] Gilad Perez,[2] Stephan Schiller,[3] Dmitry Budker,[1,4] and Dionysios Antypas[5,1,*]

[1]*Johannes Gutenberg-Universität Mainz, Helmholtz-Institut Mainz, GSI Helmholtzzentrum für Schwerionenforschung, 55128 Mainz, Germany*

[2]*Department of Particle Physics and Astrophysics, Weizmann Institute of Science, Rehovot 761001, Israel*

[3]*Heinrich-Heine-Universität Düsseldorf, 40225 Düsseldorf, Germany*

[4]*Department of Physics, University of California, Berkeley, California 94720, USA*

[5]*Department of Physics, University of Crete, 70013 Heraklion-Crete, Greece*

(Received 12 December 2022; accepted 23 May 2023; published 22 June 2023)

The effects of scalar and pseudoscalar ultralight bosonic dark matter (UBDM) were searched for by comparing the frequency of a quartz oscillator to that of a hyperfine-structure transition in ^{87}Rb, and an electronic transition in ^{164}Dy. We constrain linear interactions between a scalar UBDM field and standard-model (SM) fields for an underlying UBDM particle mass in the range 1×10^{-17}–8.3×10^{-13} eV and quadratic interactions between a pseudoscalar UBDM field and SM fields in the range 5×10^{-18}–4.1×10^{-13} eV. Within regions of the respective ranges, our constraints on linear interactions significantly improve on results from previous, direct searches for oscillations in atomic parameters, while constraints on quadratic interactions surpass limits imposed by such direct searches as well as by astrophysical observations.

DOI: 10.1103/PhysRevLett.130.251002

Introduction.—Apparently, dark matter (DM) makes up the majority of matter in our Universe [1], as indicated by decades of astronomical and cosmological observations [2], and yet the nature and composition of DM remain unknown. There is a broad class of well-motivated models, where the DM constituent is a spin-0 particle with mass in the range of $m_\phi \approx 10^{-22}$–10 eV [2,3]. These ultralight bosonic dark matter (UBDM) particles are predicted to behave locally like a classical field, coherently oscillating at the particle's Compton frequency $f_C = m_\phi/(2\pi)$.

The interaction between the UBDM field and the standard-model (SM) fields varies between different models, according to the UBDM symmetry properties such as *CP* (see Ref. [4] for a recent discussion). The UBDM particle could be a parity-even scalar field (dilaton), associated with spontaneous breaking of the scale-invariance symmetry (see for example Refs. [5,6]). Alternatively, it could be a relaxion, a special kind of axionlike particle, that couples to SM matter, dominantly, via its mixing with the Higgs boson [7–10]. Interestingly, even in the celebrated case of the *CP*-odd QCD axion [11–13], originally proposed to explain the smallness of *CP* violation in the strong force [14–21], there are quadratic-scalar interactions between the QCD-axion field and the SM ones [22]. Further exotic models dominated by a quadratically coupled UBDM were recently described in Ref. [4].

An interaction between an ultralight scalar field and SM fields may induce violation of Einstein's equivalence principle (EP) [23,24] and oscillations in the fundamental constants (FCs) of nature [5,8]. Such FCs include the fine-structure constant α, electron mass m_e, and constants which determine the nuclear mass, for instance, the QCD energy scale Λ_{QCD} and the quark masses. For a QCD-axion UBDM, oscillating nucleon electric-dipole moments are expected in the case of linear coupling, [25], and, as pointed out recently [22], oscillations in nuclear parameters such as nucleon masses and nuclear g factors are also predicted due to the presence of quadratic coupling (see also Ref. [26] for discussion on oscillating FCs due to quadratic coupling to the SM fields).

Experiments designed to check for EP violation offer a way to probe scalar UBDM [27–30]. Other works aim to detect the effects of light scalar fields by searching for oscillations in FCs. These would appear as oscillations in the length or density of solids, or in the energies of atomic or molecular levels. Various searches were proposed or completed [31–52]; see Ref. [53] for a review of experimental activities. Pseudoscalar UBDM may also introduce oscillatory effects in atomic or molecular systems [22,26], yielding observables that are indistinguishable from these due to scalar UBDM. This enables one to probe both classes of UBDM models with the same apparatus.

Here we search for the effects of scalar UBDM in two distinct experiments, where we compare the frequency of a quartz oscillator to the frequency of either of two radio-frequency (rf) transitions: a hyperfine transition

between electronic ground levels in ^{87}Rb (Experiment 1), and an electric-dipole transition between two nearly degenerate states in ^{164}Dy (Experiment 2). These searches are implemented in the UBDM particle mass range $m_\phi \approx 1 \times 10^{-17}$–$8.3 \times 10^{-13}$ eV. Part of this range has thus far remained comparatively unexplored for scalar UBDM, since it is out of reach for both state-of-the-art optical atomic clock searches (e.g., Refs. [43,44]) and a search with a gravitational-wave detector [38]. In addition to scalar UBDM, we search for pseudoscalar UBDM in the range $m_\phi \approx 5 \times 10^{-18}$–$4.1 \times 10^{-13}$ eV employing the sensitivity of Experiment 1 to the QCD axion and improving over the results of previous laboratory searches in a part of this mass range.

UBDM detection approach.—In the presence of scalar UBDM-SM interactions which are first order in the UBDM field [54], FCs such as α, m_e, and $\Lambda_{\rm QCD}$ may acquire time-dependent components:

$$\alpha(t) = \alpha_0\left[1 + d_e\frac{\phi(t)}{M_{\rm Pl}}\right], \tag{1}$$

$$m_e(t) = m_{e,0}\left[1 + d_{m_e}\frac{\phi(t)}{M_{\rm Pl}}\right], \tag{2}$$

$$\Lambda_{\rm QCD}(t) = \Lambda_{\rm QCD,0}\left[1 + d_g\frac{\phi(t)}{M_{\rm Pl}}\right]. \tag{3}$$

Here $m_{e,0}$, α_0, and $\Lambda_{\rm QCD,0}$ are the time-averaged values of the constants, $\phi(t) = \phi_0 \sin(2\pi f_C t)$ is the UBDM field of amplitude $\phi_0 = m_\phi^{-1}\sqrt{2\rho_{\rm DM}}$, where $\rho_{\rm DM} \approx 3 \times 10^{-6}$ eV^4 is the estimated local Galactic UBDM density [2], $M_{\rm Pl} = \sqrt{\hbar c/8\pi G_N} = 2.4 \times 10^{18}$ GeV is the reduced Planck mass (with G_N being the Newtonian gravitational constant), and d_e, d_{m_e}, and d_g are the respective couplings.

If instead, UBDM is due to the pseudoscalar QCD-axion field, because of axion-pion mixing, the oscillating axion background is expected to induce a temporal dependence of the pion mass [55], and thus add an oscillating component to the nucleon masses and the nuclear g factor [22]. In this case, the proton mass m_p, and the nuclear g factor for ^{87}Rb ($g_{\rm nuc}$) can be written as [22,56,57]

$$m_p(t) = m_{p,0}\left[1 - \frac{6.6 \times 10^{-3}}{f_\phi^2}\phi(t)^2\right], \tag{4}$$

$$g_{\rm nuc}(t) = g_{\rm nuc,0}\left[1 + \frac{2.6 \times 10^{-3}}{f_\phi^2}\phi(t)^2\right], \tag{5}$$

where $m_{p,0}$, $g_{\rm nuc,0}$ are the time-averaged values of the parameters, and $1/f_\phi$ is the QCD-axion coupling with the SM gluon fields, with f_ϕ being the QCD-axion decay constant.

The essence of our UBDM detection approach is to compare the frequencies of two systems (atomic vs acoustic resonance) that depend on oscillating parameters differently. Generally, a change of a constant λ by $\delta\lambda$ may change the resonance frequency f_i by δf_i, which can be quantified with a sensitivity coefficient $K_i^\lambda = (\delta f_i/f_i)/(\delta\lambda/\lambda_0)$ [63]. In frequency comparison of two systems i and j, done for example by tuning one frequency close to the other, so that $f_i \approx f_j = f$, the difference $\delta f = \delta f_i - \delta f_j$ will also change with $\delta\lambda$ as long as the two oscillators exhibit different sensitivity to λ. The fractional change can be written as $\delta f/f = (K_i^\lambda - K_j^\lambda)\delta\lambda/\lambda_0$, or assuming n FCs changing

$$\frac{\delta f}{f} = \sum_n (K_i^{\lambda_n} - K_j^{\lambda_n})\frac{\delta\lambda_n}{\lambda_{0,n}}. \tag{6}$$

Equation (6) is applied in comparing the frequency f_Q of a quartz-crystal oscillator to i) the ground-state hyperfine resonance frequency $f_{\rm HF}$ in ^{87}Rb (comparison 1) and ii) the frequency $f_{\rm Dy}$ of an rf electronic transition in ^{164}Dy (comparison 2). The relevant sensitivity coefficients are given in Table I.

The quartz frequency f_Q depends on α, m_e, and the nuclear mass $m_N \propto A \cdot \Lambda_{\rm QCD}$ [46], where A is the mass number. An atomic hyperfine frequency $f_{\rm HF}$ depends primarily on α, m_e, and $m_p \propto \Lambda_{\rm QCD}$ but with different sensitivities compared with f_Q. Thus, comparison 1 allows one to probe oscillations of α, m_e, and $\Lambda_{\rm QCD}$ within the assumption of scalar couplings. (The frequency $f_{\rm HF}$ depends additionally on the quark masses with sensitivity coefficients $\ll 1$ [64]; these contributions are omitted here.) Comparison 1 is one of the few ways to probe oscillations of the nuclear mass [51,52], and it extends the investigated frequency range for FC oscillations of a previous search based on a H maser-quartz comparison [46]. In contrast to Ref. [46], experimental sensitivity in probing FC oscillations via the Rb-quartz comparison is not limited by technical noise in the high end of the investigated frequency range, thus allowing for a more sensitive search. Applying Eq. (6) with the use of Eqs. (1)–(3) and the values in Table I, one obtains for the fractional frequency oscillations due to a scalar UBDM field

TABLE I. Assumed fractional sensitivities of oscillator-transition frequencies to different FCs, relevant for scalar and pseudoscalar interactions.

	Scalar			Pseudoscalar		
	K^α	K^{m_e}	$K^{\Lambda_{\rm QCD}}$	K^{m_p}	$K^{g_{\rm nuc}}$	References
Quartz	2	3/2	−1/2	−1/2	⋯	[46]
^{87}Rb	4.34	2	−1	−1	1	[64]
^{164}Dy	2.6×10^6	1	⋯	⋯	⋯	[65]

$$\frac{\delta f_{\mathrm{HF}}-\delta f_Q}{f}=2.34\frac{\delta\alpha}{\alpha_0}+\frac{1}{2}\frac{\delta m_e}{m_{e,0}}-\frac{1}{2}\frac{\delta\Lambda_{\mathrm{QCD}}}{\Lambda_{\mathrm{QCD},0}}=\left(2.34d_e+\frac{1}{2}d_{m_e}-\frac{1}{2}d_g\right)\frac{\phi(t)}{M_{\mathrm{Pl}}}. \quad (7)$$

We further consider comparison 1 via the quadratic coupling of the QCD-axion field, and make use of Eqs. (4) and (5) and Table I to write Eq. (6) as

$$\frac{\delta f_{\mathrm{HF}}-\delta f_Q}{f}=\frac{\delta g_{\mathrm{nuc}}}{g_{\mathrm{nuc},0}}-\frac{1}{2}\frac{\delta m_p}{m_{p,0}}=\frac{5.9\times10^{-3}}{f_\phi^2}\phi(t)^2. \quad (8)$$

We see that, due to the quadratic coupling of $\phi(t)$, oscillations of $\delta f/f$ would appear at twice the UBDM particle's Compton frequency.

If no oscillations of $\delta f/f$ are detected, Eq. (7) can be used to constrain the couplings d_{e}, $d_{\mathrm{m_e}}$, d_{g} for scalar UBDM, and Eq. (8) can be used to constrain the coupling $1/f_\phi$ for QCD-axion UBDM. Note that, although $1/f_\phi$ and m_ϕ are related for the QCD axion [14–21], here we treat them as independent quantities and estimate the reach of the experiment within a more general class of models.

In comparison 2, we benefit from using an electronic transition in Dy exhibiting extreme sensitivity to changes of α. The transition is between two nearly degenerate, excited energy levels: the $4f^9 5d^2 6s$ and $4f^{10}5d6s$ levels. Primarily due to the small transition frequency f_{Dy} (754 MHz in ^{164}Dy) and significant relativistic effects, the transition has large fractional sensitivity to α changes [65–67]. It has been employed for searches of linear-in-time drift of α and α oscillations [40] on timescales from several seconds to years. Here we extend the search in the previous work [40], primarily addressing a frequency range for the FC oscillations (100 mHz–200 Hz) that was not explored in Ref. [40]. We focus on scalar UBDM and oscillations of α, and write, analogously to Eq. (7),

$$\frac{\delta f_{\mathrm{Dy}}-\delta f_Q}{f}\approx 2.6\times10^6\frac{\delta\alpha}{\alpha_0}=2\times10^6 d_e\frac{\phi(t)}{M_{\mathrm{Pl}}}. \quad (9)$$

Since Dy sensitivity to α is vastly larger than that of quartz, comparison 2 has practically no dependence on the quartz frequency oscillating with α.

Apparatus.—In both experiments, spectroscopy of the respective rf transitions is implemented, probing atoms with a rf field produced from a quartz oscillator. The apparatus are described in detail in the Supplemental Material [57].

Apparatus 1 implements vapor-cell-based spectroscopy of the ^{87}Rb hyperfine transition, employing the optical-microwave double-resonance technique [68,69]. A Rb transition is excited with a microwave field produced by mixing the output of a commercial 100-MHz, oven-controlled, stress-compensated (SC)-cut quartz oscillator

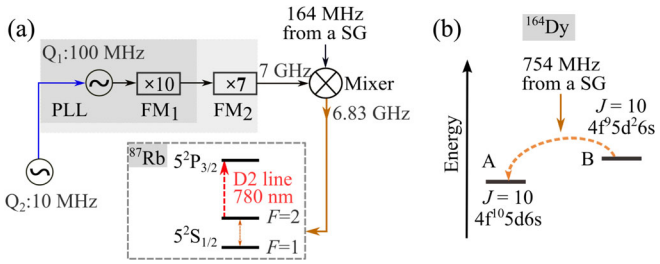

FIG. 1. (a) Schematic of the setup to produce the rf signal probing the ^{87}Rb hyperfine transition at 6.83 GHz. (b) The electric-dipole rf transition between the excited ^{164}Dy levels "B" and "A", both having the same angular momentum J. Abbreviations: PLL, phase-locked loop; FM, frequency multipliers; SG, signal generator.

(Q_1 in Fig. 1), multiplied to 7 GHz, with the signal from a function generator. The resulting frequency is close to the hyperfine-resonance frequency of ≈6.83 GHz. To reduce low-frequency noise, the oscillator Q_1 is phase locked to another oscillator (Q_2 in Fig. 1), that exhibits higher long-term frequency stability compared with Q_1. The oscillator Q_2 is also commercial, oven controlled, and constructed around a SC-cut, quartz crystal. The phase-locked loop has a measured bandwidth of ≈3 Hz. Thus, for $f_{\mathrm{C}} \leq 3$ Hz the dependence on the oscillating parameters (α, m_{e}, and m_{N}) is determined by Q_2, and for $f_{\mathrm{C}} > 3$ Hz by Q_1. The same dependence on the FCs is assumed for both.

Experiment 2 utilizes an atomic beam setup for spectroscopy of the Dy rf transition (see Ref. [70] and references therein). The atoms are prepared in the metastable state $4f^9 5d^2 6s$ (labeled "B" in Fig. 1) via a two-step laser excitation and subsequent decay [57]. The signal from a signal generator at ≈754 MHz is used to produce an electric field that induces transitions to the $4f^{10}5d6s$ state (state "A"), whose subsequent decay is monitored via fluorescence as a means to observe the $B \to A$ transition, with an observed linewidth of ≈50 kHz. The time base for the generator is provided by an internal oven-controlled, SC-cut, quartz oscillator.

Frequency-modulation spectroscopy [68] is implemented in both experiments, to improve detection sensitivity of the atomic excitations. For this, the respective rf drive is modulated in frequency, and phase-sensitive detection of the spectroscopy signal is done.

Data acquisition and analysis.—In the two experiments, the spectroscopy signal was repetitively acquired for several values of the rf-modulation frequency. In apparatus 1, we found that the experimental parameters providing optimal sensitivity are different for different ranges of the frequency f_{C} (see the Supplemental Material [57]). Thus, in the low-frequency run, we recorded many 4-h-long time series for a total of 600 h, with a sampling rate of 41.7 Sa/s, while in the high-frequency run, we acquired a sequence of 10-min-long time series, for a total of 144 h, sampling the signal at 406.5 Sa/s. The data taken for Experiment 2 were a

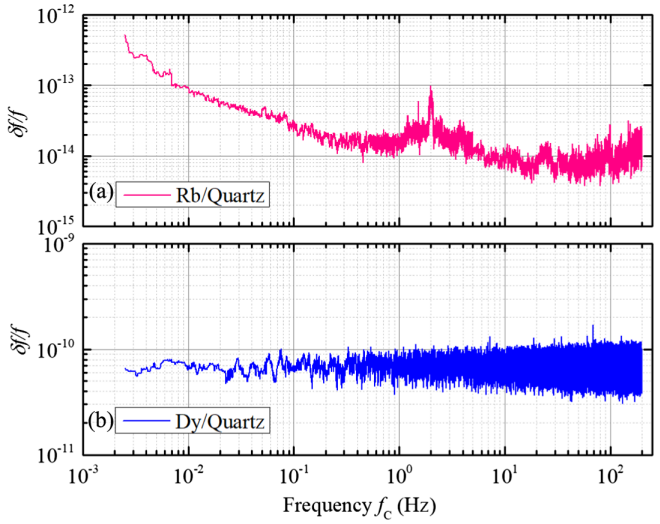

FIG. 2. Exclusion limits on fractional frequency oscillations $\delta f/f$ at 95% C.L. (a) Experiment 1. The spectrum is produced by merging the spectra from the low- and high-frequency runs at 5 Hz, i.e., the frequency where the respective FC detection sensitivities become equal. We do not provide limits in the frequency windows 50 ± 0.25 Hz and 100 ± 0.25 Hz. (b) Experiment 2. The spectrum exhibits no pronounced dependence on frequency, as the dominant noise source is shot noise in the detection of Dy transitions in the atomic beam.

total of 12 h, with the spectroscopy signal sampled at 406.5 Sa/s and recorded in three successive, 4-h-long time series.

From the recorded time series, power spectra were computed and averaged. The corresponding amplitude spectra were investigated for possible signatures of oscillations that would appear as amplitudes in frequency bins of the spectra, that are greater than a threshold for detection. This threshold is determined by the random noise in the vicinity of the bins, and set to a 95% confidence level, accounting for the look-elsewhere effect [71] (see the Supplemental Material [57]). We checked this set threshold by injecting artificial signals to the recorded time series, and looking at the size of the respective amplitudes in the computed spectra (see the Supplemental Material [57]).

A total of ten peaks was observed to exceed the threshold for detection in the low-frequency run of Experiment 1, and 231 peaks were seen in the high-frequency run. In Experiment 2, 983 peaks were observed. All these spurious signals were checked via (i) intercomparison of the averaged amplitude spectra acquired with different modulation frequencies, (ii) cross-checks between the spectra acquired for the low- and high-frequency range runs (relevant in Experiment 1), and (iii) comparison of primary datasets against sets from auxiliary runs with an alternative signal generator (see Fig. 1). As an actual UBDM signal should persist in all these tests, eventually all spurious peaks were excluded from being UBDM candidates, allowing us to constrain the spectra of the fractional frequency oscillations $\delta f/f$, as shown in Fig. 2 [72].

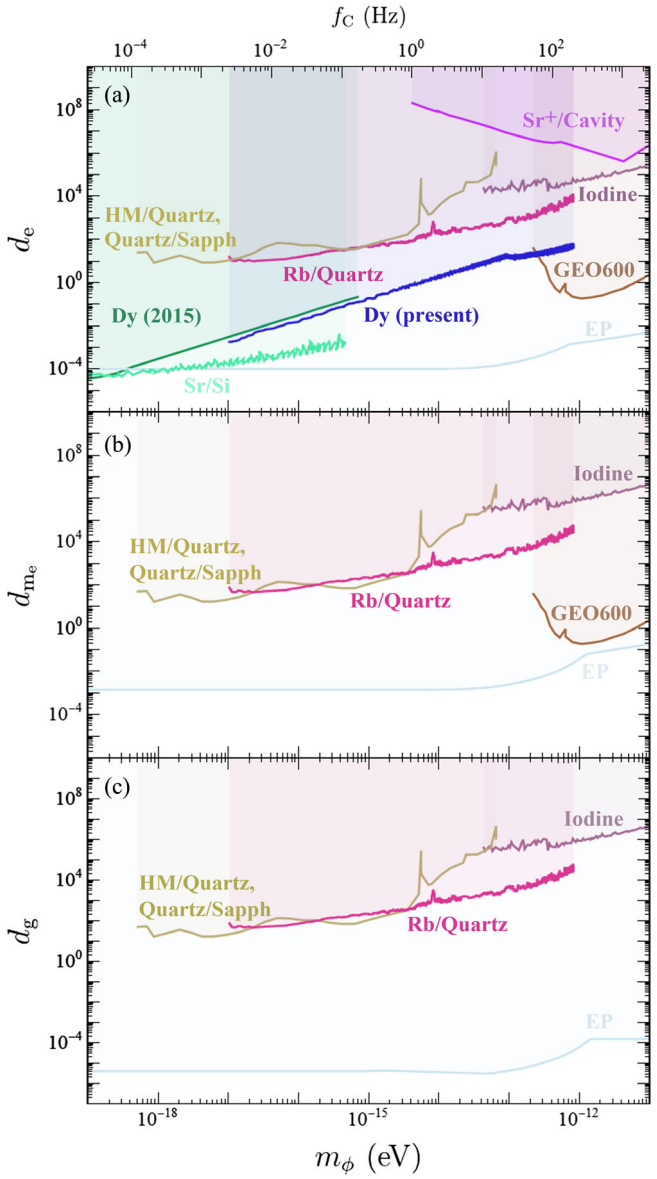

FIG. 3. Constraints on the UBDM couplings to (a) α, (b) m_e, and (c) Λ_{QCD} from the present work (Rb/quartz and Dy/quartz), shown at the 95% C.L., alongside constraints from other experiments. Dy (2015), Ref. [40]; Sr lattice clock-Si optical cavity (Sr/Si), Ref. [44]; Sr^+ optical clock transition-optical cavity (Sr^+/cavity), Ref. [45]; iodine, Ref. [52]; GEO600, Ref. [38]; H maser-quartz & quartz-cryogenic sapphire oscillator (HM/quartz-quartz/sapph), Ref. [46]; EP, Refs. [78–80]. The limits from Ref. [46] are plotted considering the respective parameters independently, and multiplying by a factor ×4.4 to account for stochasticity of UBDM in that work, as it was done for the Rb/quartz and Dy/quartz data (see text).

Constraints on UBDM couplings.—We use the constraints on $\delta f/f$ (Fig. 2) and Eqs. (6), (7), and (9) to bound the UBDM couplings to α, m_e, and Λ_{QCD} (Fig. 3). To do this, we assume that the respective coupling dominates the UBDM-SM interaction. In addition, we consider the stochastic nature of the UBDM field [73] and apply a

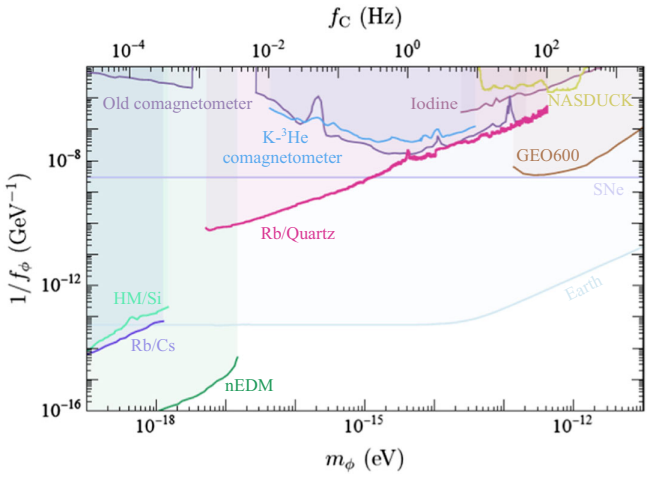

FIG. 4. Constraints on the QCD axion-gluon coupling. Rb/Cs [41], hydrogen maser-silicon optical cavity (HM/Si) [44], neutron EDM (nEDM) [85], iodine [52], GEO 600 [38], supernovae (SNe) [84], old comagnetometer [82], NASDUCK [83], K-^{3}He comagnetometer [86], Earth-induced QCD axion density effect (Earth) [87].

correction to the bounds to account for the reduction in UBDM detection sensitivity that becomes appreciable at oscillation frequencies $f_C < Q/T$ [74], where $Q \approx 1.1 \times 10^6$ is the Q factor of the UBDM field within the standard Galactic UBDM halo scenario [75], and T is the total measurement time; $T = 864$ h and 12 h for Experiments 1 and 2, respectively. Applying the analysis method of Ref. [76] we find that the bounds from Experiments 1 and 2 become weaker by a factor of ≈4.4 below ≈1 Hz and ≈50 Hz, respectively [77].

The bounds on d_e, d_{m_e}, and d_g from the Rb/quartz comparison improve on previous results by as many as ×100 times in the range 1–200 Hz. Within the whole range investigated (2.5 mHz–200 Hz), a variety of experiments directly probe for oscillations of α and m_e, as seen in Figs. 3(a) and 3(b). Few experiments however, probe a hyperfine resonance (as we do in this Letter), and are sensitive to oscillations of the strong force [Fig. 3(c)].

A more stringent bound on d_e is provided by the Dy experiment. The limit $\delta f/f \approx 8 \times 10^{-11}$ translates to a limit of $\delta\alpha/\alpha \approx 3 \times 10^{-17}$ and a bound on d_e that improves on previous results by as many as 3 orders of magnitude, despite the relatively short 12-h-long data taking [81]. Having UBDM detection capability up to the frequency of the observed transition linewidth (≈50 kHz) Experiment 2 is used to explore a region between the upper-frequency end in state-of-the-art atomic clock searches (e.g., Ref. [44]) and the low-frequency end of the GEO600 search [38].

The assumption of pseudoscalar UBDM allows one to interpret the $\delta f/f$ limits from Experiment 1 as limits on the QCD axion-gluon coupling $1/f_\phi$ (Fig. 4) via Eq. (8). Here as well a correction is made to account for the stochasticity of UBDM; it amounts to a calculated degradation of the limit of Fig. 2 by a factor of ≈2.5 in the sub-Hz region. Our constraints on $1/f_\phi$ (Fig. 2) improve on those from tabletop experiments probing the effects of an axion coupling via atomic magnetometry [82,83]. They also surpass astrophysical limits [84] in the frequency range below 200 mHz.

Conclusions and outlook.—Our bounds on scalar and pseudoscalar UBDM interactions represent significant improvement over previous work in part of the explored mass range. While the limits on scalar couplings to the α, m_e, and d_g from EP-violation searches are more stringent, direct searches for oscillations in these constants offer important cross-checks. In addition, as discussed in Refs. [4,52], if the scalar UBDM has some nongeneric coupling to the SM, then bounds from the EP-violation-fifth-force experiments may be suppressed by a factor $\mathcal{O}(10^3)$ and may become comparable to that of FC-oscillation searches [48].

The recent work [22] pointing to oscillatory effects in nuclear parameters in the presence of the QCD axion, extends the physics reach of apparatus used thus far to check for FC oscillations. As we show here, this opens a way to probe pseudoscalar UBDM with sensitivity that is, in a certain mass range, far greater than that in setups designed to search for previously considered pseudoscalar-field observables.

This possibility motivates further apparatus improvements, for example, in probing the hyperfine resonance. The present Rb/quartz frequency comparison is at the $10^{-12}/\sqrt{\tau}$ level in the short term (measurement time $\tau < 10$ s); this is ≈10 times lower than that reported for a vapor-cell-based Rb clock [88]. Long-term stability can be improved by optimization of the parameters of the Rb-vapor-cell setup [88]. Because the stability of a quartz oscillator degrades at such long timescales, it would be necessary to replace it with a microwave signal derived from an optical atomic clock or an optical cavity [44]. Together with a long data-taking campaign, such improvements could extend the reach of an experiment by orders of magnitude, and probe for the QCD axion further beyond the level allowed by atomic magnetometry and astrophysical observations.

We thank W. Ji for discussions and N. L. Figueroa, D. Kanta, U. Rosowski, and M. Hansen for help with the project. This work was supported by the European Research Council (ERC) under the European Union Horizon 2020 research and innovation program (project YbFUN, Grant Agreement No. 947696) and by the DFG Project ID 390831469: EXC 2118 (PRISMA + Cluster of Excellence). This Letter is based in part upon the work from COST Action COSMIC WISPers CA21106, supported by COST (European Cooperation in Science and Technology). The work of A. B. is supported by the Azrieli Foundation.

*dantypas@physics.uoc.gr

[1] R. L. Workman *et al.* (Particle Data Group), Review of particle physics, Prog. Theor. Exp. Phys. **2022**, 083C01 (2022).

[2] *The Search for Ultralight Bosonic Dark Matter*, edited by D. F. Jackson Kimball and K. van Bibber (Springer, New York, 2023).

[3] M. S. Safronova, D. Budker, D. DeMille, Derek F. Jackson Kimball, A. Derevianko, and C. W. Clark, Search for new physics with atoms and molecules, Rev. Mod. Phys. **90**, 025008 (2018).

[4] A. Banerjee, G. Perez, M. S. Safronova, I. Savoray, and A. Shalit, The phenomenology of quadratically coupled ultra light dark matter, arXiv:2211.05174.

[5] A. Arvanitaki, J. W. Huang, and K. Van Tilburg, Searching for dilaton dark matter with atomic clocks, Phys. Rev. D **91**, 015015 (2015).

[6] W. Graham, P. G. Irastorza, I. K. Lamoreaux, S, A. Lindner, and K. A. Van Bibber, Experimental searches for the axion and axion-like particles, Annu. Rev. Nucl. Part. Sci. **65**, 485 (2015).

[7] P. W. Graham, D. E. Kaplan, and S. Rajendran, Cosmological Relaxation of the Electroweak Scale, Phys. Rev. Lett. **115**, 221801 (2015).

[8] A. Banerjee, H. J. Kim, and G. Perez, Coherent relaxion dark matter, Phys. Rev. D **100**, 115026 (2019).

[9] T. Flacke, C. Frugiuele, E. Fuchs, R. S. Gupta, and G. Perez, Phenomenology of relaxion-Higgs mixing, J. High Energy Phys. 17 (2017) 50.

[10] A. Banerjee, H. J. Kim, O. Matsedonskyi, G. Perez, and M. S. Safronova, Probing the relaxed relaxion at the luminosity and precision frontiers, J. High Energy Phys. 07 (2020) 153.

[11] J. Preskill, M. B. Wise, and Frank Wilczek, Cosmology of the invisible axion, Phys. Lett. **120B**, 127 (1983).

[12] L. F. Abbott and P. Sikivie, A cosmological bound on the invisible axion, Phys. Lett. **120B**, 133 (1983).

[13] M. Dine and W. Fischler, The not so harmless axion, Phys. Lett. **120B**, 137 (1983).

[14] R. D. Peccei and Helen R. Quinn, Constraints imposed by *CP* conservation in the presence of instantons, Phys. Rev. D **16**, 1791 (1977).

[15] R. D. Peccei and Helen R. Quinn, *CP* Conservation in the Presence of Instantons, Phys. Rev. Lett. **38**, 1440 (1977).

[16] S. Weinberg, A New Light Boson?, Phys. Rev. Lett. **40**, 223 (1978).

[17] F. Wilczek, Problem of Strong *P* and *T* Invariance in the Presence of Instantons, Phys. Rev. Lett. **40**, 279 (1978).

[18] J. E. Kim, Weak Interaction Singlet and Strong *CP* Invariance, Phys. Rev. Lett. **43**, 103 (1979).

[19] M. A. Shifman, A. I. Vainshtein, and V. I. Zakharov, Can confinement ensure natural *CP* invariance of strong interactions?, Nucl. Phys. **B166**, 493 (1980).

[20] A. R. Zhitnitsky, On possible suppression of the axion hadron interactions (In Russian), Sov. J. Nucl. Phys. **31**, 260 (1980).

[21] M. Dine, W. Fischler, and M. Srednicki, A simple solution to the strong *CP* problem with a harmless axion, Phys. Lett. **104B**, 199 (1981).

[22] H. J. Kim and G. Perez, Oscillations of atomic energy levels induced by QCD axion dark matter, arXiv:2205.12988.

[23] T. Damour and J. F. Donoghue, Equivalence principle violations and couplings of a light dilaton, Phys. Rev. D **82**, 084033 (2010).

[24] A. Hees, O. Minazzoli, E. Savalle, Y. V. Stadnik, and P. Wolf, Violation of the equivalence principle from light scalar dark matter, Phys. Rev. D **98**, 064051 (2018).

[25] P. W. Graham and S. Rajendran, New observables for direct detection of axion dark matter, Phys. Rev. D **88**, 035023 (2013).

[26] Y. V. Stadnik and V. V. Flambaum, Can Dark Matter Induce Cosmological Evolution of the Fundamental Constants of Nature?, Phys. Rev. Lett. **115**, 201301 (2015).

[27] G. L. Smith, C. D. Hoyle, J. H. Gundlach, E. G. Adelberger, B. R. Heckel, and H. E. Swanson, Short-range tests of the equivalence principle, Phys. Rev. D **61**, 022001 (1999).

[28] S. Schlamminger, K.-Y. Choi, T. A. Wagner, J. H. Gundlach, and E. G. Adelberger, Test of the Equivalence Principle Using a Rotating Torsion Balance, Phys. Rev. Lett. **100**, 041101 (2008).

[29] P. Touboul *et al.*, Microscope Mission: First Results of a Space Test of the Equivalence Principle, Phys. Rev. Lett. **119**, 231101 (2017).

[30] J. Bergé, P. Brax, G. Métris, M. Pernot-Borràs, P. Touboul, and J. P. Uzan, Microscope Mission: First Constraints on the Violation of the Weak Equivalence Principle by a Light Scalar Dilaton, Phys. Rev. Lett. **120**, 141101 (2018).

[31] A. Arvanitaki, S. Dimopoulos, and K. Van Tilburg, Sound of Dark Matter: Searching for Light Scalars with Resonant-Mass Detectors, Phys. Rev. Lett. **116**, 031102 (2016).

[32] J. Manley, D. J. Wilson, R. Stump, D. Grin, and S. Singh, Searching for Scalar Dark Matter with Compact Mechanical Resonators, Phys. Rev. Lett. **124**, 151301 (2020).

[33] A. A. Geraci, C. Bradley, D. F. Gao, J. Weinstein, and A. Derevianko, Searching for Ultralight Dark Matter with Optical Cavities, Phys. Rev. Lett. **123**, 031304 (2019).

[34] Y. V. Stadnik and V. V. Flambaum, Searching for Dark Matter and Variation of Fundamental Constants with Laser and Maser Interferometry, Phys. Rev. Lett. **114**, 161301 (2015).

[35] Y. V. Stadnik and V. V. Flambaum, Enhanced effects of variation of the fundamental constants in laser interferometers and application to dark-matter detection, Phys. Rev. A **93**, 063630 (2016).

[36] H. Grote and Y. V. Stadnik, Novel signatures of dark matter in laser-interferometric gravitational-wave detectors, Phys. Rev. Res. **1**, 033187 (2019).

[37] E. Savalle, A. Hees, F. Frank, E. Cantin, P. E. Pottie, B. M. Roberts, L. Cros, B. T. McAllister, and P. Wolf, Searching for Dark Matter with an Optical Cavity and an Unequal-Delay Interferometer, Phys. Rev. Lett. **126**, 051301 (2021).

[38] S. M. Vermeulen *et al.*, Direct limits for scalar field dark matter from a gravitational-wave detector, Nature (London) **600**, 424 (2021).

[39] L. Aiello, J. W. Richardson, S. M. Vermeulen, H. Grote, C. Hogan, O. Kwon, and C. Stoughton, Constraints on Scalar Field Dark Matter from Colocated Michelson Interferometers, Phys. Rev. Lett. **128**, 121101 (2022).

[40] K. Van Tilburg, N. Leefer, L. Bougas, and D. Budker, Search for Ultralight Scalar Dark Matter with Atomic Spectroscopy, Phys. Rev. Lett. **115**, 011802 (2015).
[41] A. Hees, J. Guéna, M. Abgrall, S. Bize, and P. Wolf, Searching for an Oscillating Massive Scalar Field as a Dark Matter Candidate Using Atomic Hyperfine Frequency Comparisons, Phys. Rev. Lett. **117**, 061301 (2016).
[42] P. Wcisło *et al.*, New bounds on dark matter coupling from a global network of optical atomic clocks, Sci. Adv. **4**, eaau4869 (2018).
[43] K Beloy *et al.*, Frequency ratio measurements at 18-digit accuracy using an optical clock network, Nature (London) **591**, 564 (2021).
[44] C. J. Kennedy, E. Oelker, J. M. Robinson, T. Bothwell, D. Kedar, W. R. Milner, G. E. Marti, A. Derevianko, and J. Ye, Precision Metrology Meets Cosmology: Improved Constraints on Ultralight Dark Matter from Atom-Cavity Frequency Comparisons, Phys. Rev. Lett. **125**, 201302 (2020).
[45] S. Aharony, N. Akerman, R. Ozeri, G. Perez, I. Savoray, and R. Shaniv, Constraining rapidly oscillating scalar dark matter using dynamic decoupling, Phys. Rev. D **103**, 075017 (2021).
[46] W. M. Campbell, B. T. McAllister, M. Goryachev, E. N. Ivanov, and M. E. Tobar, Searching for Scalar Dark Matter via Coupling to Fundamental Constants with Photonic, Atomic, and Mechanical Oscillators, Phys. Rev. Lett. **126**, 071301 (2021).
[47] D. Antypas, O. Tretiak, A. Garcon, R. Ozeri, G. Perez, and D. Budker, Scalar Dark Matter in the Radio-Frequency Band: Atomic-Spectroscopy Search Results, Phys. Rev. Lett. **123**, 141102 (2019).
[48] O. Tretiak, X. Zhang, N. L. Figueroa, D. Antypas, A. Brogna, A. Banerjee, G. Perez, and D. Budker, Improved Bounds on Ultralight Scalar Dark Matter in the Radio-Frequency Range, Phys. Rev. Lett. **129**, 031301 (2022).
[49] V. V. Flambaum, A. J. Mansour, I. B. Samsonov, and C. Weitenberg, Searching for scalar field dark matter with hyperfine transitions in alkali atoms, Phys. Rev. D **107**, 015008 (2023).
[50] D. Hanneke, B. Kuzhan, and A. Lunstad, Optical clocks based on molecular vibrations as probes of variation of the proton-to-electron mass ratio, Quantum Sci. Technol. **6**, 014005 (2020).
[51] D. Antypas, O. Tretiak, K. Zhang, A. Garcon, G. Perez, M. G. Kozlov, S. Schiller, and D. Budker, Probing fast oscillating scalar dark matter with atoms and molecules, Quantum Sci. Technol. **6**, 034001 (2021).
[52] R. Oswald *et al.*, Search for Dark-Matter-Induced Oscillations of Fundamental Constants Using Molecular Spectroscopy, Phys. Rev. Lett. **129**, 031302 (2022).
[53] D Antypas *et al.*, New horizons: Scalar and vector ultralight dark matter, arXiv:2203.14915
[54] See Refs. [4,24] for phenomenology of second-order couplings.
[55] L. Ubaldi, Effects of theta on the deuteron binding energy and the triple-alpha process, Phys. Rev. D **81**, 025011 (2010).
[56] V. V. Flambaum and A. F. Tedesco, Dependence of nuclear magnetic moments on quark masses and limits on temporal variation of fundamental constants from atomic clock experiments, Phys. Rev. C **73**, 055501 (2006).
[57] See Supplemental Material at http://link.aps.org/supplemental/10.1103/PhysRevLett.130.251002 for the derivation of the coefficients, which includes Refs. [58,59], as well as the details of Experiment 2, which includes Refs. [60–62].
[58] P. Di Vecchia and G. Veneziano, Chiral dynamics in the large n limit, Nucl. Phys. **B171**, 253 (1980).
[59] C. Vafa and E. Witten, Parity Conservation in QCD, Phys. Rev. Lett. **53**, 535 (1984).
[60] A. T. Nguyen, G. D. Chern, D. Budker, and M. Zolotorev, Efficient population transfer in a multilevel system using diverging laser beams, Phys. Rev. A **63**, 013406 (2000).
[61] A. Cingoz, A laboratory test of Einstein's equivalence principle in atomic dysprosium: Search for temporal and gravitational variation of the fine-structure constant, Ph.D. thesis, University of California, Berkeley, 2019.
[62] D. Budker, D. DeMille, E. D. Commins, and M. S. Zolotorev, Experimental investigation of excited states in atomic dysprosium, Phys. Rev. A **50**, 132 (1994).
[63] M. G. Kozlov and D. Budker, Comment on sensitivity coefficients to variation of fundamental constants, Ann. Phys. (Amsterdam) **531**, 1800254 (2019).
[64] V. V. Flambaum, D. B. Leinweber, A. W. Thomas, and R. D. Young, Limits on variations of the quark masses, QCD scale, and fine structure constant, Phys. Rev. D **69**, 115006 (2004).
[65] V. A. Dzuba, V. V. Flambaum, and M. V. Marchenko, Relativistic effects in Sr, Dy, Yb II, and Yb III and search for variation of the fine-structure constant, Phys. Rev. A **68**, 022506 (2003).
[66] V. A. Dzuba, V. V. Flambaum, and J. K. Webb, Calculations of the relativistic effects in many-electron atoms and space-time variation of fundamental constants, Phys. Rev. A **59**, 230 (1999).
[67] V. A. Dzuba and V. V. Flambaum, Relativistic corrections to transition frequencies of Ag I, Dy I, Ho I, Yb II, Yb III, Au I and Hg II and search for variation of the fine-structure constant, Phys. Rev. A **77**, 012515 (2008).
[68] W. Demtröder, *Laser Spectroscopy*, 5th ed. (Springer, Berlin-Heidelberg, 2015), Vol. 2.
[69] T Bandi, C Affolderbach, and G Mileti, Laser-pumped paraffin-coated cell rubidium frequency standard, J. Appl. Phys. **111**, 124906 (2012).
[70] N. Leefer, C. T. M. Weber, A. Cingoz, J. Torgerson, and D. Budker, New Limits on Variation of the Fine-Structure Constant Using Atomic Dysprosium, Phys. Rev. Lett. **111**, 060801 (2013).
[71] J. D. Scargle, Studies in astronomical time series analysis. II. Statistical aspects of spectral analysis of unevenly spaced data, Astrophys. J. **263**, 835 (1982).
[72] It is challenging to reliably compute a threshold for detection of oscillation in the $\delta f/f$ spectra for $f_C < 1$ mHz (see the Supplemental Material [57]). Here we provide constraints for $f_C \geq 2.5$ mHz.
[73] G. P. Centers *et al.*, Stochastic fluctuations of bosonic dark matter, Nat. Commun. **12**, 7321 (2021).
[74] To within a factor of 2π [75].
[75] A. V. Gramolin, A. Wickenbrock, D. Aybas, H. Bekker, D. Budker, G. P. Centers, N. L. Figueroa, D. F. Jackson

Kimball, and A. O. Sushkov, Spectral signatures of axion-like dark matter, Phys. Rev. D **105**, 035029 (2022).
[76] B. E. J. Pelssers, Enhancing direct searches for dark matter, Ph.D. thesis, Stockholm University, Sweeden, 2022.
[77] This ≈4.4 correction factor may be conservative, compared with the factor ≈3 of [73].
[78] P. Touboul, G. Metris, M. Rodrigues, Y. Andre, Q. Baghi *et al.*, MICROSCOPE Mission: First Results of a Space Test of the Equivalence Principle, Phys. Rev. Lett. **119**, 231101 (2017).
[79] T. A. Wagner, S. Schlamminger, J. H. Gundlach, and E. G. Adelberger, Torsion-balance tests of the weak equivalence principle, Classical Quantum Gravity **29**, 184002 (2012).
[80] G. L. Smith, C. D. Hoyle, J. H. Gundlach, E. G. Adelberger, Blayne R. Heckel, and H. E. Swanson, Short range tests of the equivalence principle, Phys. Rev. D **61**, 022001 (1999).
[81] Since sensitivity in probing FC oscillations scales as $\sim 1/\sqrt{\tau}$ (τ is the measurement time), further data taking would yield moderate improvement. Considering the challenges with operating the Dy atomic beam apparatus continuously, a more efficient approach to enhance DM-detection sensitivity is to improve apparatus signal-to-noise ratio. Related apparatus upgrades are underway.
[82] I. M. Bloch, Y. Hochberg, E. Kuflik, and T. Volansky, Axion-like relics: New constraints from old comagnetometer data, J. High Energy Phys. 01 (2020) 167.
[83] I. M. Bloch, G. Ronen, R. Shaham, O. Katz, T. Volansky, and O. Katz (NASDUCK Collaboration), New constraints on axion-like dark matter using a Floquet quantum detector, Sci. Adv. **8**, abl8919 (2022).
[84] G. G. Raffelt, Astrophysical axion bounds, Lect. Notes Phys. **741**, 51 (2008).
[85] C. Abel, N. J. Ayres, G. Ban, G. Bison, K. Bodek *et al.*, Search for Axionlike Dark Matter through Nuclear Spin Precession in Electric and Magnetic Fields, Phys. Rev. X **7**, 041034 (2017).
[86] J. Y. Lee, M. Lisanti, W. A. Terrano, and M. Romalis, Laboratory Constraints on the Neutron-Spin Coupling of feV-Scale Axions, Phys. Rev. X **13**, 011050 (2023).
[87] A. Hook and J. W. Huang, Probing axions with neutron star inspirals and other stellar processes, J. High Energy Phys. 06 (2018) 036.
[88] T. Bandi, C. Affolderbach, C. Stefanucci, F. Merli, A. K. Skrivervik, and G. Mileti, Compact high-performance continuous-wave double-resonance rubidium standard with 1.4×10^{-13} $\mathrm{T}^{-1/2}$ stability, IEEE Trans. Ultrason. Ferroelectr. Freq. Control **61**, 1769 (2014).